AMERICAN SOCIETY FOR MICROBIOLOGY | mSphere®

RESEARCH ARTICLE

Cyanophage Diversity and Community Structure in Dead Zone Sediments

Elias Broman,[a,b] Karin Holmfeldt,[c] Stefano Bonaglia,[a,d,e] Per O. J. Hall,[e] Francisco J. A. Nascimento[a,b]

[a]Department of Ecology, Environment and Plant Sciences, Stockholm University, Stockholm, Sweden
[b]Baltic Sea Centre, Stockholm University, Stockholm, Sweden
[c]Centre for Ecology and Evolution in Microbial Model Systems (EEMiS), Linnaeus University, Kalmar, Sweden
[d]Department of Biology, University of Southern Denmark, Nordcee and HADAL, Odense, Denmark
[e]Department of Marine Sciences, University of Gothenburg, Gothenburg, Sweden

ABSTRACT Up to 20% of prokaryotic organisms in the oceans are estimated to die every day due to viral infection and lysis. Viruses can therefore alter microbial diversity, community structure, and biogeochemical processes driven by these organisms. Cyanophages are viruses that infect and lyse cyanobacterial cells, adding bioavailable carbon and nutrients into the environment. Cyanobacteria are photosynthesizing bacteria, with some species capable of N_2 fixation, which are known to form large blooms as well as resistant resting cells known as akinetes. Here, we investigated cyanophage diversity and community structure plus cyanobacteria in dead zone sediments. We sampled surface sediments and sequenced DNA and RNA, along an oxygen gradient—representing oxic, hypoxic, and anoxic conditions—in one of the world's largest dead zones located in the Baltic Sea. Cyanophages were detected at all stations and, based on partial genome contigs, had a higher alpha diversity and different beta diversity in the hypoxic-anoxic sediments, suggesting that cyanobacteria in dead zone sediments and/or environmental conditions select for specific cyanophages. Some of these cyanophages can infect cyanobacteria with potential consequences for gene expression related to their photosystem and phosphate regulation. Top cyanobacterial genera detected in the anoxic sediment included *Dolichospermum*/*Anabaena*, *Synechococcus*, and *Cyanobium*. RNA transcripts classified to cyanobacteria were associated with numerous pathways, including anaerobic carbon metabolism and N_2 fixation. Cyanobacterial blooms are known to fuel oxygen-depleted ecosystems with phosphorus (so-called internal loading), and our cyanophage data indicate the potential for viral lysis of cyanobacteria which might explain the high nutrient turnover in these environments.

IMPORTANCE Cyanophages are viruses that target cyanobacteria and directly control their abundance via viral lysis. Cyanobacteria are known to cause large blooms in water bodies, substantially contributing to oxygen depletion in bottom waters resulting in areas called dead zones. Our knowledge of cyanophages in dead zones is very scarce, and so far, no studies have assembled partial cyanophage genomes and investigated their associated cyanobacteria in these dark and anoxic sediments. Here, we present the first study using DNA and RNA sequencing to investigate *in situ* diversity of cyanophages and cyanobacteria in dead zones. Our study shows that dead zone sediments contain different cyanophages compared to oxic sediments and suggest that these viruses are able to affect cyanobacterial photosystem and phosphate regulation. Furthermore, cyanophage-controlled lysis of cyanobacteria might also increase the turnover of carbon, phosphorus, and nitrogen in these oxygen-free environments at the bottom of the sea.

KEYWORDS DNA, anoxic, cyanobacteria, cyanophages, sediment, virus

Citation Broman E, Holmfeldt K, Bonaglia S, Hall POJ, Nascimento FJA. 2021. Cyanophage diversity and community structure in dead zone sediments. mSphere 6:e00208-21. https://doi.org/10.1128/mSphere.00208-21.

Editor Yonghua Li-Beisson, Aix-Marseille University

Address correspondence to Elias Broman, elias.broman@su.se.

Received 8 March 2021
Accepted 1 April 2021
Published 28 April 2021

Viruses are up to 15-fold more abundant than prokaryotic organisms, and up to 20% of all microorganisms in the oceans are estimated to die daily because of viral infection and lysis (1). Viruses are therefore able to alter microbial diversity, community structure, and biogeochemical processes driven by these microorganisms (1). Among viruses with important ecosystem effects are cyanophages. These viruses are known to infect cyanobacteria, and after infection, lytic cyanophages eventually lyse the host cell (2–4) and thus contribute to the release of carbon and nutrients into the environment (5, 6). Many cyanobacterial species are capable of photosynthesis and N_2 fixation (7) and are therefore essential primary producers channeling organic carbon and nitrogen to higher trophic levels in both aquatic and terrestrial ecosystems (8–12). While some cyanobacteria, such as the genus *Synechococcus*, have been shown to proliferate in oligotrophic waters (13), other genera, e.g., *Aphanizomenon*, *Nodularia*, and *Dolichospermum* (previously classified as planktonic *Anabaena* [14]), form large blooms in aquatic systems during high-nutrient-load—yet nitrogen-limited—and warm periods (15, 16). A portion of these blooms eventually decay and sink down below the euphotic zone and settle on the seabed (15, 17, 18). Cyanophages can increase the decay of these pelagic cyanobacteria while sinking down toward the seabed through increased particle formation caused by viral lysis (19). On the sediment surface, the settled cyanobacterial bloom material provides organic matter for benthic consumers and adds to the internal loading of phosphorus in the system (8, 12, 20, 21). Eventually, microbial degradation of this material and other sources of organic matter together with water stratification depletes oxygen in the bottom water, and so-called hypoxic ($<63\,\mu$M O_2) or anoxic "dead zones" are formed (17, 22). As a result of eutrophication, dead zones can today be found in coastal areas adjacent to all populated continents (23) and consist of habitats rich in organic carbon and ammonium. In addition to sinking decaying blooms, cyanobacteria can also sink to the sediment as resting cells called akinetes that tolerate harsh conditions (24). Cyanobacteria are also known to survive these dead zones despite darkness (25, 26) and anoxic conditions (27) and might therefore be infected by cyanophages in dead zone sediments.

One of the largest dead zones in the world is located in the Baltic Sea (23), which hosts large cyanobacterial blooms in the surface water during summer (28), and anoxic waters below a permanent oxycline situated at 65- to 125-m depth (29). Viruses have been shown to be active and persist in sediment for thousands of years (30, 31). For example, Cai et al. (31) showed that cyanophages persist for centuries in dead zones in the Baltic Sea, indicating that cyanophages are present in the sediment in addition to newly recruited phages associated with sinking cyanobacteria. Cyanobacterial blooms have been traced back to ca. 7,000 years ago in the Baltic Sea (based on pigment analysis in deep sediments) (32), and it is therefore likely that the ancient cyanophages are remnants from these sinking blooms. Considering that cyanophages lyse cyanobacterial cells that release bioavailable carbon and nutrients (5), cyanophages might have a key role in the food web of dead zone sediments. Even though it is known that cyanophages are present in dead zones, there is a knowledge gap regarding their diversity, community composition, and associated cyanobacteria.

Here, we aimed to elucidate the role of *in situ* cyanophages and cyanobacteria in dead zone sediments. To investigate this aim, we sampled the top 0- to 2-cm sediment surface from four stations along a 60- to 210-m water depth gradient in one of the largest dead zones in the world (the Baltic Sea). These stations included oxic (station A), hypoxic (D), near-anoxic (E), and anoxic (F) sediment (Table 1; oxygen data first reported in the work of Broman et al. [33]). In addition to the oxygen gradient, stations D and F have been reported to have higher concentrations of toxic hydrogen sulfide (H_2S), and station E higher concentrations of nitrous oxide (N_2O) (33). DNA and RNA were extracted and sequenced using the latest sequencing technology (Illumina NovaSeq) to investigate cyanophages and cyanobacteria. We hypothesized that (i) the diversity and community structure of cyanophages are different along the oxic-anoxic

TABLE 1 Sampling conditions[a]

Station	Water depth (m)	O_2 (μmol liter^{-1})	Date	Longitude	Latitude
A	60	330	April 25	19°04′951	57°23′106
D	130	8.8	April 26	19°19′414	57°19′671
E	170	1.8	April 23	19°30′451	57°07′518
F	210	0	April 23	19°48′035	57°17′225

[a]Triplicate sediment samples (top 0- to 2-cm sediment surface) were collected during 2018 in the Eastern Gotland basin dead zone in the Baltic Sea. The stations were located along a water depth gradient (all aphotic) with different bottom water oxygen conditions. Oxygen concentrations shown were measured in the top 0- to 0.5-mm sediment surface, with station A being oxic, D hypoxic, E near-anoxic, and F anoxic. Oxygen data were first reported in the work of Broman et al. (33).

biogeochemical gradient and (ii) any such difference is linked to changes in cyanobacterial community composition and RNA transcripts.

RESULTS

Cyanophage diversity and community composition. A total of 90 partial cyanophage genomes (i.e., contigs) were assembled from the coassembly metagenome data with an average genome size of 5,076 bp (range 2,000 to 47,157 bp). These partial cyanophage genome sequences were used in network analyses using vConTACT (34), which clusters genome-wide proteins based on the Markov Cluster Algorithm (MCL), and showed that the cyanophages formed three clusters (Fig. 1). These clusters were similar to *Siphoviridae* cyanophages (x), *Podoviridae* cyanophages (y), and *Myoviridae* cyanophages (z) (according to the cyanophage taxonomic classifications) (Fig. 1). See Fig. S1 in the supplemental material for the whole vConTACT network analysis including all reference viruses. Of these 90 identified cyanophages, 77 had a mapped read coverage of at least 75% and were therefore considered to be present in the sediment at the stations (Fig. 2 and see Data Set S1 for a full list of the cyanophages and their classified closest relative according to NCBI NT).

Shannon's H alpha diversity was higher for cyanophage contigs in the dead zone sediment, with: 3.07 ± 0.11 (station D, $P = 0.081$), 3.51 ± 0.43 (E, $P = 0.007$), and 3.11 ± 0.39 (F, $P = 0.067$) compared to 2.37 ± 0.11 at station A [$n = 3$ per station, 1 standard deviation shown, one-way analysis of variance (ANOVA) with Tukey *post hoc* test, whole model $F_{(3,8)} = 7.39$, $P = 0.011$; Fig. 2]. In addition, the community composition of the cyanophage contigs was different in oxic sediment at station A compared to the hypoxic-anoxic sediment at stations D, E, and F (Bray-Curtis beta diversity, permutational multivariate analysis of variance [PERMANOVA], $_{pseudo}F = 5.71$, $P = 0.0006$; Fig. 2). There was also a significant difference in Bray-Curtis beta diversity excluding the oxic station A, with the anoxic station F clustering differently from the stations D and E (PERMANOVA, $_{pseudo}F = 1.75$, $P = 0.03$; Fig. S2). A similar pattern with higher alpha diversity and different community structure in the dead zone sediment was also observed when analyses were conducted on the classified taxonomy of the contigs (Fig. S3). These differences in cyanophage alpha and beta diversity are also visible in Fig. 2, and interestingly most cyanophage contigs with a high relative abundance in the oxic sediment at station A belonged to cluster x, while cyanophages in the hypoxic-anoxic sediment mainly belonged to clusters y and z (Fig. 3).

Cyanobacterial diversity and taxonomy. Cyanobacteria were detected in all metagenome and transcriptome sequencing (RNA-seq) sediment samples at all stations ($n = 3$ per station for both DNA and RNA data). The number of classified reads belonging to cyanobacteria was on average 3.3% (range 2.5 to 4.5%) in the DNA data and showed a decreasing trend along water depth (i.e., oxic station A to anoxic station F) from 7.9 to 4.2% (Fig. S4) in the RNA data. Both the cyanobacterial DNA and RNA data sets were dominated by populations belonging to the oxygenic photosynthetic class *Oxyphotobacteria*, with especially two taxonomic orders: (i) *Synechococcales* (up to 65% of the cyanobacteria in the RNA data) and (ii) *Nostocales* (up to 44% of the cyanobacteria in the RNA data; Fig. 4A). In the DNA data, there was an increasing pattern of reads

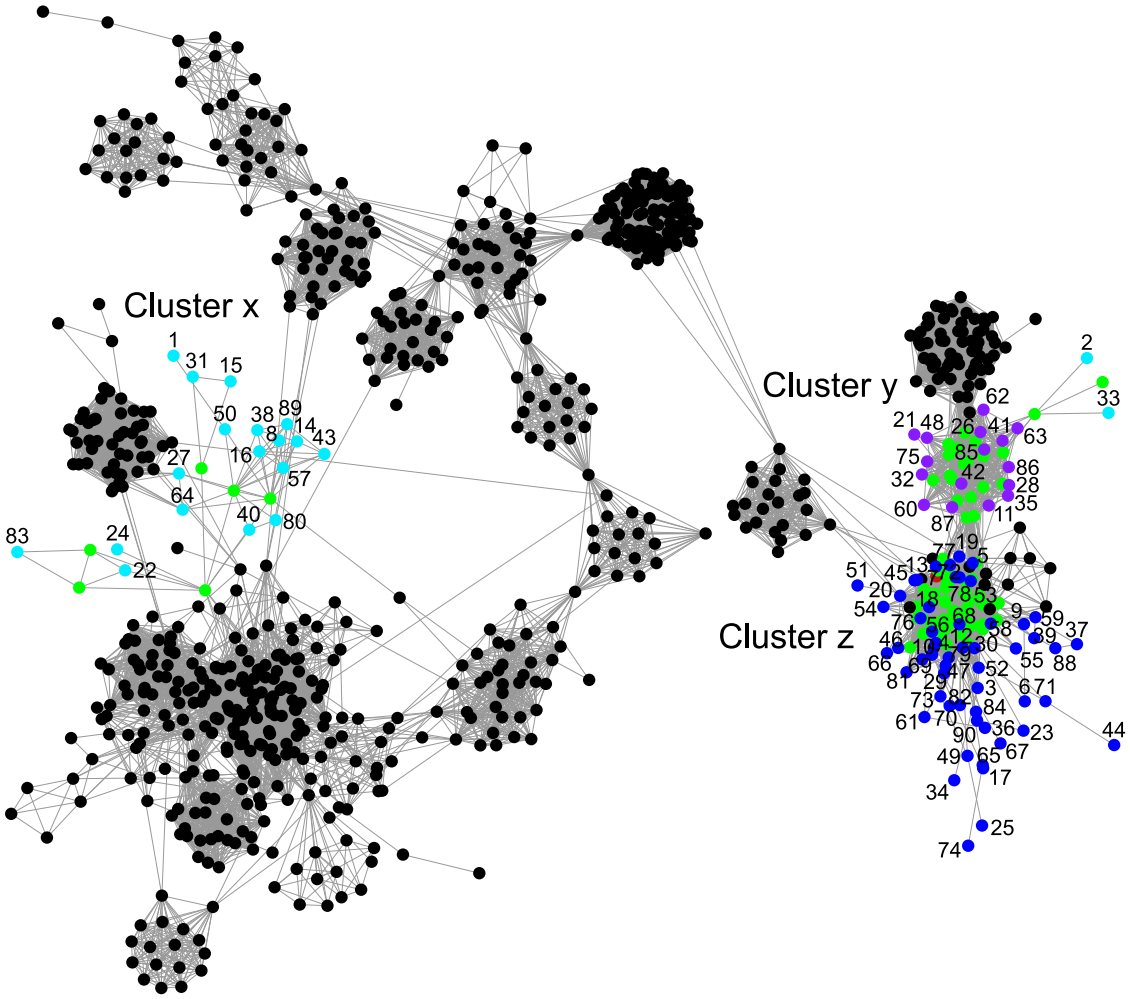

FIG 1 Network analysis consisting of reference viruses (NCBI bacterial and archaeal viral RefSeq V88) and the constructed virus contigs. The black nodes show noncyanophage viruses from the reference database, while green nodes show known cyanophages. The constructed contigs classified as viruses by VirSorter and associated with cyanophages in the vConTACT network analysis are denoted as turquoise, purple, and blue nodes (followed by the contig ID number) and clustered into three groups in the network (x, y, and z). Color codes: turquoise, cyanophages belonging to the family *Siphoviridae*; purple, *Podoviridae*; blue, *Myoviridae*; red, no taxonomic classification.

classified to *Nostocales*, from 13% to 33% of all cyanobacteria, along the water depth gradient (i.e., stations A to F; Fig. 4A). Looking closer at the cyanobacteria in the hypoxic-anoxic sediment (stations D, E, and F), most of the classified reads were attributed to (i) the genera *Cyanobium* and *Synechococcus*, both belonging to the order *Synechococcales* (both in the DNA and RNA data), and (ii) the genus *Anabaena* belonging to the order *Nostocales* (15 to 20% of all cyanobacteria; mainly in the RNA data; Fig. 4B). Note that the reference database (NCBI RefSeq) might still label some species of *Dolichospermum* as *Anabaena*. *Cyanobium* was attributed more DNA and RNA-seq classified reads at the oxic station A than at the hypoxic-anoxic stations D, E, and F, with DNA 51% and RNA 14% of all cyanobacteria compared to DNA 14% and RNA 5%, respectively. *Synechococcus* showed the opposite pattern with higher numbers of reads at stations D, E, and F (DNA 19% and RNA 16% of all cyanobacteria compared to station A with DNA 12% and RNA 11%; Fig. 4B). These results indicate that cyanobacteria, even bloom-forming oxygenic photosynthetic taxa, are present and transcribe genes (as indicated in the mRNA data) in the dead zone sediment. A full list of read counts and sequence classifications against cyanobacterial genomes in the RefSeq database is available in Data Set S2.

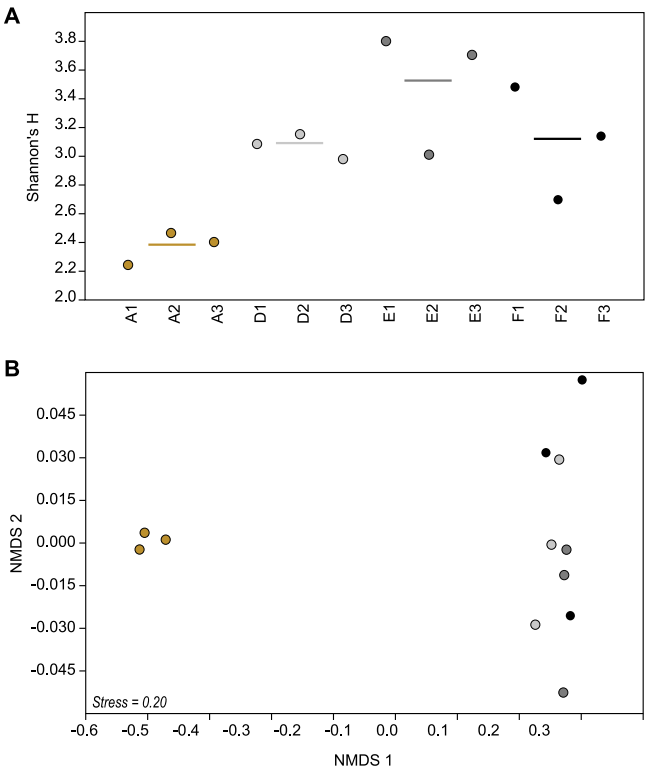

FIG 2 (A) Alpha diversity (Shannon's H) of cyanophage contigs present in the samples (with at least 75% mapped read coverage). The bars show average values per station. (B) NMDS showing Bray-Curtis beta diversity of the cyanophages between the stations. The colors denote the different stations as follows: brown, A (oxic); light gray, D (hypoxic); dark gray, E (near-anoxic); and black, F (anoxic).

Cyanobacterial alpha diversity (Shannon's H) in the sediment was significantly higher in the oxic station A (Shannon's H 4.17 $\pm$ 0.02) than in the hypoxic-anoxic stations D, E, and F [Shannon's H 3.92 to 3.94; one-way ANOVA, $F_{(3,8)} = 129.76$, $P < 0.001$; and Tukey *post hoc* tests $P < 0.001$].

Cyanophages and associated cyanobacteria in the dead zone sediments. The community compositions of the cyanophage contigs in the sediment were found to largely cluster with stations D and E. Similarly, the composition of cyanobacteria formed three clusters, stations D + E, A, and F, which were in relation to the oxygen concentrations at the stations (RNA data; Fig. 5A). The cyanophage contigs distributed in the sediments also showed an association with the cyanobacterial proteins. Here, cyanophage contigs x16, x27, x57, z7, z79, and z81 occurring at the oxic station A (Fig. 3) clustered toward the beta diversity of the UniProtKB/Swiss-Prot classified cyanobacterial proteins (mRNA data) in the sediment of station A (Fig. 5B). The majority of the cyanophage contigs and cyanobacterial proteins clustered with the hypoxic-anoxic stations (right side in Fig. 5B). BVSTEP analysis showed that the combination of the three cyanophage contigs y2, x16, and z58 best explained the beta diversity of the cyanobacterial proteins (rho = 0.80). That the cyanophages had an effect on the cyanobacterial community in the hypoxic-anoxic sediment was also indicated by several cyanophage contigs (z5, z10, z12, z13, z17, z19, z45, z46, y48, z58, z74, z76, z78, and z82) correlating positively with the number of mapped RNA transcripts attributed to cyanobacterial protein CRISPR-associated endoribonuclease Cas2 3 (gene *cas2-3*; rho = 0.60 to 0.86, $n = 12$ for each cyanophage, all $P < 0.05$; Fig. 5C). Finally, the taxonomy and protein classifications of the cyanophage contigs revealed that the majority were identified to genomes of *Synechococcus* or *Prochlorococcus* phages in the database (Data

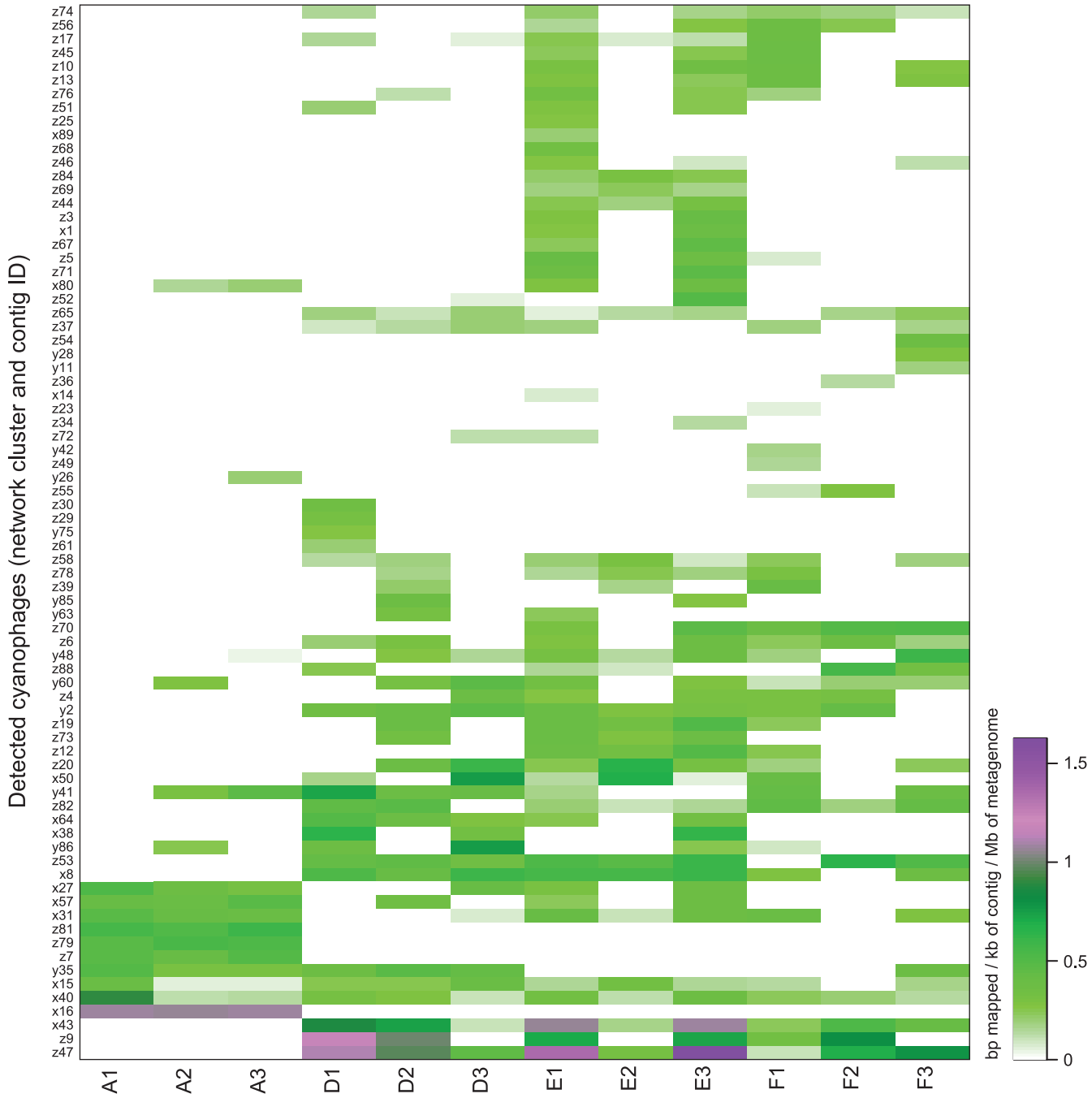

FIG 3 One-way clustered heatmap by rows showing cyanophage constructed contigs with a minimum of 75% coverage. The green-purple color gradient shows normalized sequence counts (mapped bp per contig/contig length in kb/metagenome in Mb). The row labels show contig IDs and their associated network cluster in Fig. 1 (x, y, or z).

Sets S1 and S3) and were carrying a large number of gene copies related to hypothetical proteins but also, e.g., glycosyl transferase-related genes, heat shock protein IbpA, p-starvation-inducible protein (gene *phoH*), and photosystem II D1 (*psbA* genes) (Data Set S3).

Cyanobacterial RNA transcripts in the dead zone sediments. The number of cyanobacterial RNA transcripts was significantly higher at station A (363 ± 45 GeTMM [*ge*ne length corrected *t*rimmed *m*ean of *M*-values]) compared to the hypoxic-anoxic stations D, E, and F (170 ± 37, 158 ± 42, and 126 ± 21, respectively; $F = 24.9$, $P < 0.001$, one-way ANOVA with Tukey *post hoc* test; Fig. 6A). RNA transcripts for the KEGG

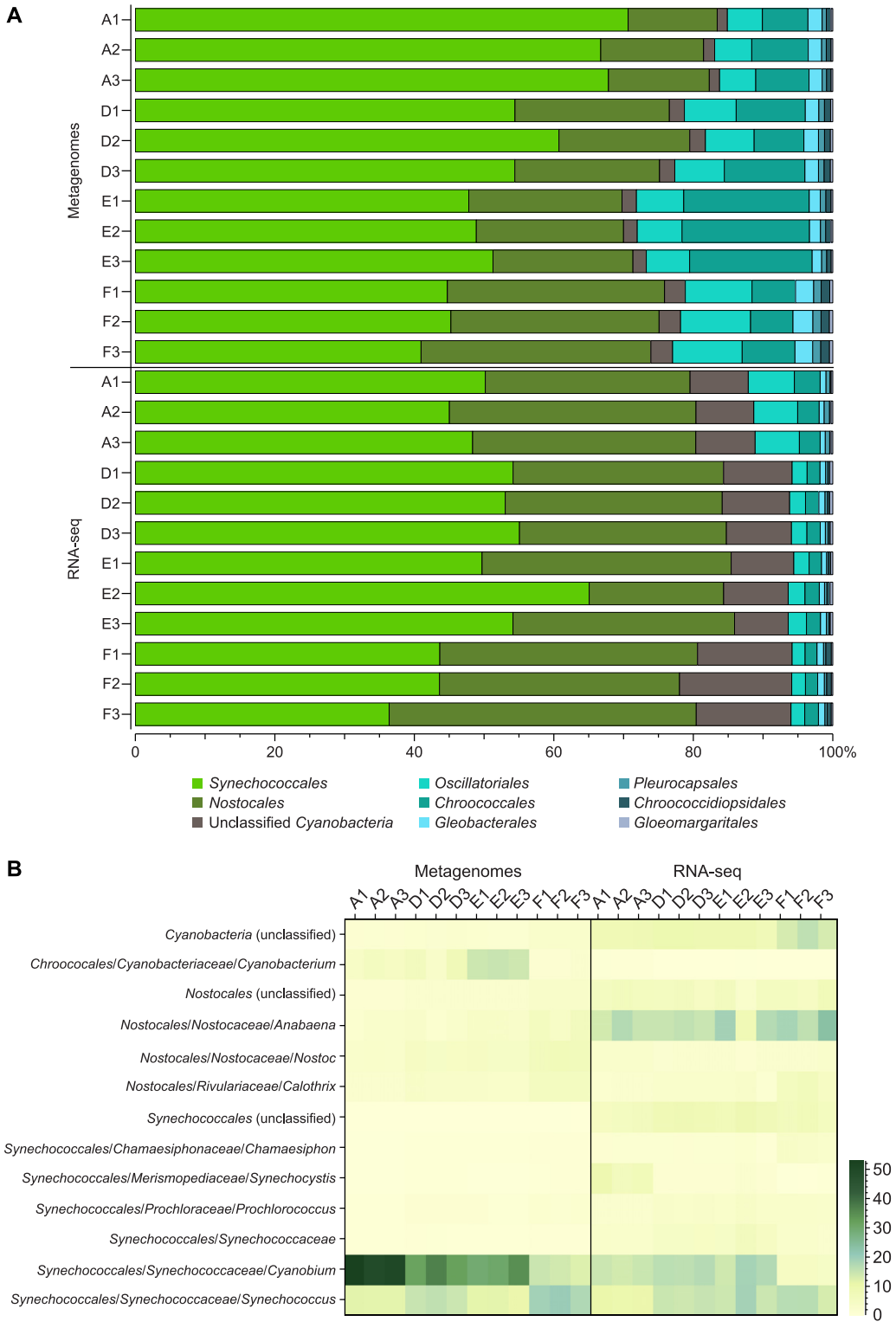

FIG 4 (A) The stacked bars show the relative proportion of classified DNA and RNA sequences against cyanobacterial genomes in the RefSeq database. The data show % of cyanobacteria, and the color legend shows taxonomic orders, while the *y* axis shows the triplicate samples for each station. (B) Heatmap showing the relative proportion of classified reads against cyanobacterial genomes in the RefSeq database. The data show the lowest taxonomic classification with at least an average of >2% in the DNA or RNA samples.

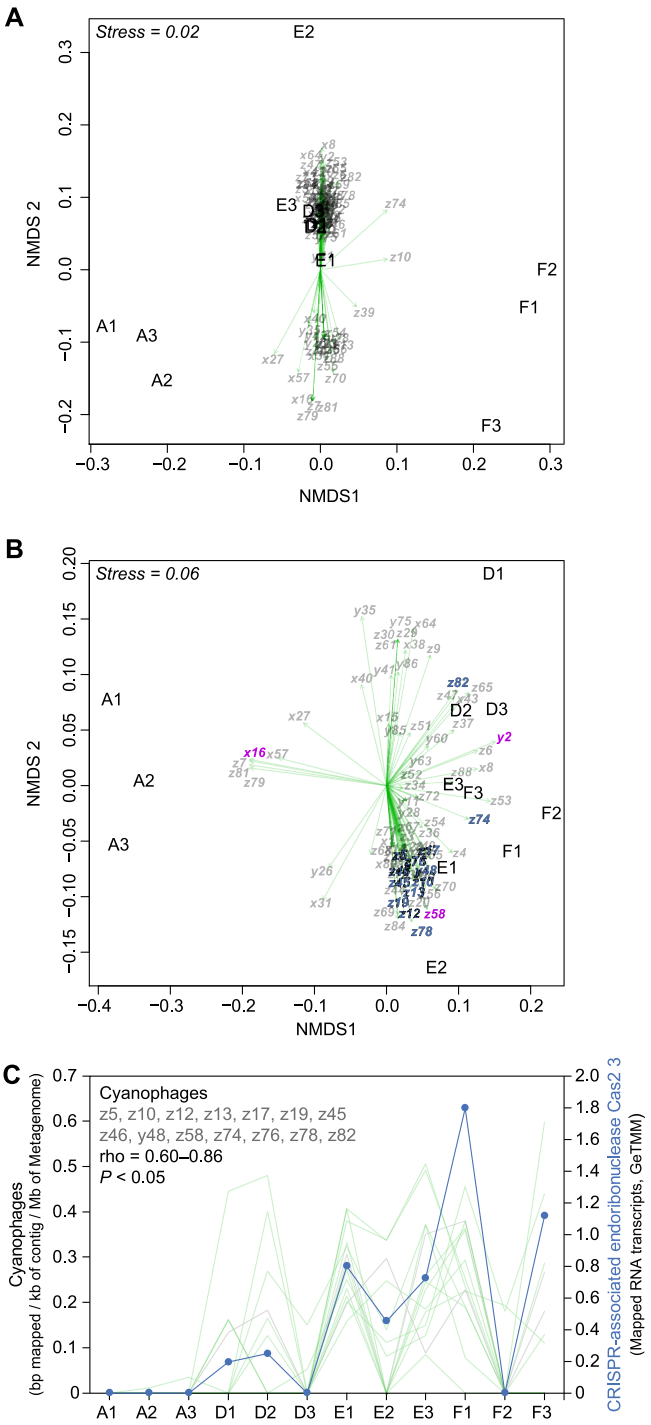

FIG 5 (A) NMDS showing the Bray-Curtis beta diversity based on the proportion of reads classified of the cyanobacterial RNA data (lowest taxonomic classification; stations shown on the graph). The overlying triplot shows the distribution of detected cyanophage contigs (light gray labels) in relation to the cyanobacterial beta diversity. The arrowheads denote the data point of the cyanophage. (B) NMDS showing the Bray-Curtis beta diversity of UniProtKB/Swiss-Prot-classified cyanobacterial proteins (mRNA data) identified in the data set (stations shown and denoted on the graph). Cyanophage contigs indicated by violet color (y2, x16, and z58) denote the cyanophages that together best explain the beta diversity of the cyanobacterial proteins (rho = 0.80). The blue cyanophage contigs (as well as violet z58) denote the cyanophage contigs in panel C that correlated with a cyanobacterium-related CRISPR protein. (C) Several of the cyanophage contigs in the hypoxic-anoxic sediment correlated positively with the number of mapped RNA transcripts against the metagenome assembly attributed to cyanobacterial protein CRISPR-associated endoribonuclease Cas2 3 (gene *cas2-3*). The light gray lines denote each cyanophage contig, while the blue line denotes the GeTMM values for the CRISPR protein.

A

KEGG MODULE	A1	A2	A3	D1	D2	D3	E1	E2	E3	F1	F2	F3
Cysteine biosynthesis	6.9	8.4	10.7	3.0	1.4	3.2	2.2	2.5	4.1	2.9	2.6	4.7
Fatty acid biosynthesis	9.0	11.6	6.9	4.1	4.0	5.1	6.7	2.7	7.2	6.5	10.6	6.8
Fatty acid biosynthesis, elongation	5.7	7.2	4.0	1.6	2.2	2.6	4.6	1.8	3.9	3.9	5.6	4.7
Fatty acid biosynthesis, initiation	3.3	5.2	2.4	1.6	2.2	2.3	2.7	2.0	2.6	3.3	1.0	1.6
F-type ATPase	4.7	9.7	5.1	4.0	6.6	5.9	2.5	3.5	4.9	3.2	3.6	8.3
Glycolysis (Embden-Meyerhof pathway)	6.1	5.7	2.7	2.5	4.8	1.5	5.6	4.0	2.9	3.7	2.1	3.5
Heme biosynthesise	4.9	7.5	4.9	4.0	5.2	6.0	12.8	4.0	5.2	9.0	3.2	7.1
NAD(P)H:quinone oxidoreductase	5.3	7.1	6.4	2.0	1.2	2.8	2.8	1.2	2.1	2.5	2.5	3.1
Nitrate assimilation	14.4	23.9	14.6	0.1	0.1	0.3	0.4	0.2	0.3	0.4	0.0	0.1
Pentose phosphate pathway (Pentose phosphate cycle)	5.8	6.8	3.4	1.3	2.1	1.6	3.0	1.7	2.0	3.4	2.3	1.8
Photosystem I	10.1	9.9	9.7	1.3	1.8	2.6	2.2	2.3	3.1	4.6	2.5	3.0
Photosystem II	136.9	140.4	110.8	55.2	90.5	68.4	51.5	28.0	71.0	3.4	1.7	5.1
Pimeloyl-ACP biosynthesis, BioC-BioH pathway	5.7	7.2	4.0	1.6	2.2	2.6	4.6	1.8	3.9	3.9	5.6	4.7
Reductive citrate cycle (Arnon-Buchanan cycle)	7.8	5.1	5.5	2.0	5.0	2.1	3.7	1.8	2.8	2.8	3.3	4.7
Reductive pentose phosphate cycle (Calvin cycle)	5.2	3.8	4.8	1.2	3.4	1.5	2.9	0.4	1.4	1.3	0.8	2.2
Siroheme biosynthesis	4.7	3.5	2.9	2.0	2.1	3.2	6.5	1.6	2.4	3.6	1.4	3.1
Tetrahydrofolate biosynthesis	4.2	4.5	2.5	1.1	1.8	1.1	2.1	1.5	2.1	2.7	3.6	2.7
Uridine monophosphate biosynthesis	12.8	7.4	15.1	3.2	2.0	2.8	2.0	0.6	0.8	1.0	1.0	0.9
Tetrahydrofolate biosynthesis, mediated by PTPS	3	4	2	1	2	1	2	2	2	3	4	3
3-Hydroxypropionate bi-cycle	3	5	2	1	2	2	2	2	3	3	1	2
									Legend	0	5	≥10

B

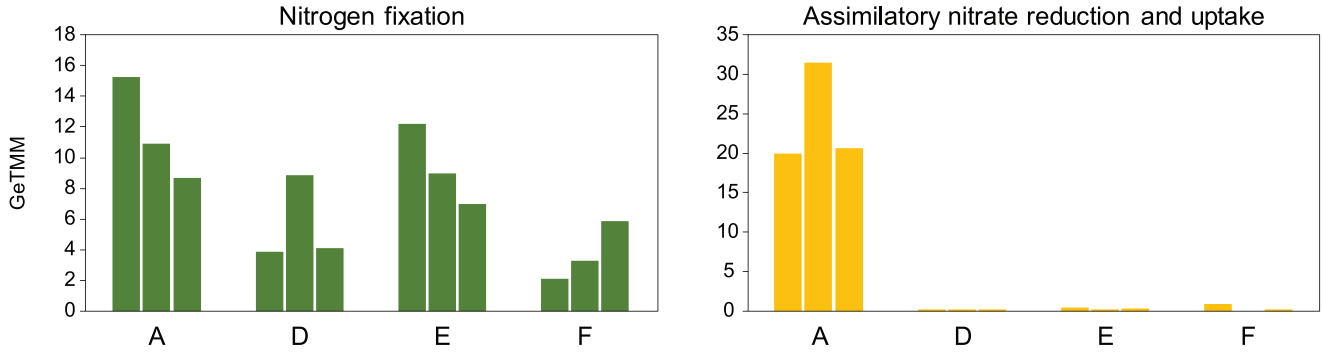

FIG 6 (A) Cyanobacterial RNA transcripts classified against the UniProtKB/Swiss-Prot linked to KEGG modules. The heatmap shows the top 20 modules and normalized sequence counts (GeTMM). Note that proteins might be associated with more than one module. (B) Cyanobacterial RNA transcripts attributed to "N_2 fixation" and "assimilatory nitrate reduction and uptake" based on UniProtKB/Swiss-Prot classifications. Note the different *y* axes between subpanels.

module glycolysis were prevalent at all stations, indicating that anaerobic carbon metabolism was likely occurring. Furthermore, RNA transcripts attributed to other KEGG modules present at all stations included, e.g., fatty acid biosynthesis, proteins that were part of the reductive citrate cycle (Arnon-Buchanan cycle), cystine amino acid synthesis, and the photosystems (Fig. 6A). Photosystem I had more RNA transcripts at station A ($F = 85.7$, $P < 0.001$), while the photosystem II had a different number of RNA transcripts for each station (when each station was tested against the others [$F = 31.3$, $P < 0.05$; Fig. 6A]). The number of RNA transcripts attributed to nitrate assimilation was significantly higher at station A than at all other stations ($F = 30.8$, $P < 0.001$; Fig. 6A). Because not all proteins could be classified into KEGG modules, we also decided to inspect the UniProtKB/Swiss-Prot-classified protein data manually. A full list of proteins affiliated with cyanobacteria, KEGG KOs plus modules, and a list of proteins with a significant difference between stations are available in Data Set S4.

RNA polymerase was present at all stations in the cyanobacterial RNA data (Data Set S4); also, the oxic station A had more RNA transcripts classified to ribosomal proteins (30S and 50S) than did the other stations under hypoxic and anoxic conditions (edgeR analysis, false-discovery rate [FDR] < 0.05). Furthermore, the number of significantly different proteins between station A and stations D, E, and F increased with water depth, with A versus D, 58 proteins; A versus E, 69 proteins; and A versus F, 90 proteins (Data Set S4). This shows that with decreasing oxygen concentrations, and increasing distance from oxic station A, the difference in cyanobacterial metabolism increases.

Cyanobacterial RNA transcripts for N_2 fixation (genes *nifDEHKNU*) were present at all stations (Fig. 6B). The number of *nifU* RNA transcripts was higher at station A than at D and F (FDR < 0.05), and *nifH* RNA transcripts were higher at station E than at station A (FDR < 0.05). Genes related to assimilatory nitrate reduction and uptake (nitrate reductase *narB* and nitrate transporters *nrtABCDP*) had together more RNA transcripts at the oxic station A than at the hypoxic-anoxic stations (20 to 30 GeTMM at station A compared to <1 GeTMM at the other stations; Fig. 6B). Of these, RNA transcripts attributed to genes *narB* and *nrtP* were significantly higher at station A (FDR < 0.05) than at stations D, E, and F (Data Set S4).

DISCUSSION

We detected cyanophages at all four stations along the oxic-anoxic gradient. Viruses in sediment are affected by water flow and environmental shifts due to seasonal changes, as well as microbial abundances and activity (35). However, dead zones in the Baltic Sea are relatively stable environments due to a strong halocline trapping the heavy, more saline and oxygen-deficient bottom water (23). In the sampled gradient, we detected that cyanophages (based on partial genome contigs and classified closest relatives according to NCBI NT) had a higher alpha diversity and different beta diversity in the hypoxic-anoxic sediment compared to the oxic station A, which confirmed our first hypothesis. This might partly be explained by a higher abundance of viruses in deep anoxic water, which has been reported in the Baltic Sea (36) and in other anoxic areas such as the Cariaco basin in the Caribbean Sea (37). In addition, cyanophages were indicated to have an association with different cyanobacterial communities and their RNA transcripts across the sampled gradient (as indicated in Fig. 5A and B), confirming our second hypothesis. This indicates that cyanobacteria in the hypoxic-anoxic sediment have to cope with a more diverse cyanophage community compared to that of the oxic sediments. Considering that cyanophages can persist for thousands of years in anoxic sediments (31), differences in the cyanophage community composition and diversity might also be an effect of accumulating viruses in dead zone sediments. Cyanobacterial CRISPR-associated endoribonuclease-related RNA transcripts (attributed to gene *cas2-3*) were correlated with the relative abundance of several cyanophages, possibly due to viral infection. On the bacterial genome, CRISPR (clustered regularly interspaced short palindromic repeats) loci consist of virus-specific DNA repeats with adjacent *cas* genes. Upon viral infection, the virus DNA is sampled and inserted into a CRISPR locus and transcribed into crRNA, which is then used to guide Cas endonuclease proteins to cleave invading virus DNA (38). Our findings suggest that cyanobacteria were targeted by cyanophages in the sampled sediments. However, we were unable to retrieve any counts after mapping the RNA data to the cyanophage genes, likely due to (i) insufficient mRNA reads, considering that any viral transcription would be very small compared to the whole RNA data set, and/or that (ii) a substantial portion of the cyanophages were present without infected hosts. It has previously been shown that cyanophages can persist for centuries in the deep anoxic Baltic Sea (37 m below the seafloor) (31), and it is therefore possible that a large portion of cyanophages were present in our sampled sediments but not infecting any host cells. Considering that our data indicate that cyanobacteria were transcribing genes in all the sampled stations, it is possible that at least some cyanophages were infecting host cells.

Viral lysis of cyanobacterial cells contributes carbon, phosphorus, and nitrogen to other microorganisms (5, 6). The bacterial uptake of lysed material has been shown to be especially important in oligotrophic environments where nutrients are scarce (39), and our results suggest that the presence of cyanophages in dead zone sediments could result in cyanobacterial lysed cells and support elevated nutrient turnover. This phage-driven lysis of cyanobacteria and consequence for nutrient turnover would, nevertheless, need to be confirmed in future studies. Cyanophages are known to carry genes for the photosystem II (40), as confirmed by our results. However, in contrast to

cyanophages that were limited to *psbA* genes, the RNA transcript data for cyanobacteria were attributed to multiple different photosynthesis-related genes (at least 30 genes detected in this study). In more detail, the cyanobacterial photosynthesis data set was dominated by *psbA* genes at all stations except the anoxic station F. It is therefore possible that changes in cyanobacterial photosynthesis regulation could have partly been due to viral infection by cyanophages. Our results indicate that prokaryote-virus interactions are an important factor to consider in future studies looking at prokaryotic photosystem genes or protein counts. Similarly, cyanophages were also found to carry genes for the phosphorus regulon *phoH*. Even though the function of the translated protein is still not fully understood (40), the transcription of the *phoH* gene has been shown to be induced by phosphate starvation (41). Cyanophages might therefore have influenced the cycling of phosphate by infecting cyanobacteria in the sediment. Further studies are needed to investigate the impact of such nutrient fluxes in dark and anoxic sediments. We were not able to determine if cyanophages influenced the community composition of the cyanobacteria (or vice versa), or how many of the assembled partial cyanophage genomes in this study were derived from sinking pelagic cyanobacteria or were already residing in the sediment. However, the difference in cyanophage alpha and beta diversity between the oxic and hypoxic-anoxic sediment suggests that (i) host-associated cyanobacteria capable of surviving in oxygen-deficient environments select for specific cyanophages and/or (ii) cyanophages in dead zones might have a lower decay rate (36) and be more tolerant to the certain environmental conditions, such as H_2S, which has been shown to have antiviral properties for respiratory viruses (42).

In addition to the cyanophages, our DNA and RNA data also show that cyanobacteria were present in the dead zone sediments. This is in agreement with previous studies showing that cyanobacteria are able to survive in dark and anoxic environments either as akinetes (24) or by utilizing fermentative metabolism (43). Furthermore, cyanobacterial RNA transcripts related to RNA processing and modification, protein biosynthesis, protein processing, and cyanobacterial cold shock protein have been detected *in situ* in the anoxic sediment at the deepest point in the Baltic Sea (Landsort deep, 466 m) (44). The presence of the filamentous genus *Anabaena* (potentially containing planktonic species belonging to the renamed *Dolichospermum* genus, and/or as benthic *Anabaena*) in our study indicated that akinetes or fermentative metabolism could have been possible. Interestingly, the relative proportion of classified reads attributed to *Anabaena* was higher in the RNA-seq than in the DNA data, and this might be explained by the following: (i) *Anabaena* is known to produce akinetes (24) and (ii) certain species of *Anabaena* are known to be heterotrophic and survive in darkness even under anaerobic conditions (43). The presence of *Anabaena* in the hypoxic-anoxic sediment could also be related to the lower rate of organic matter degradation in oxygen-deficient sediments (45, 46), resulting in pelagic cyanobacterial material being likely preserved for a considerable time. However, RNA transcript data directly affiliated with cyanobacteria suggest that at least some of these organisms are actively transcribing genes in dead zone sediments. *Anabaena* might use fermentative metabolism (endo- or exogenous [43]) or akinete resting stages (with a low metabolic signal that was present in the RNA data). For example, the species *Anabaena cylindrica* has been observed to produce H_2 by utilizing endogenous substrates (47). In contrast to *Anabaena*, the other top genera detected in the hypoxic-anoxic sediment *Cyanobium* and *Synechococcus* are not known to form akinetes (48). However, *Synechococcus* has been shown to survive in anoxic and dark waters in the Black Sea with strong indications of being capable of fermentation (49). Our mRNA data further suggest that these cyanobacteria are present in dark and anoxic environments.

The mRNA data from cyanobacteria in the hypoxic-anoxic sediment also indicate that N_2-fixation genes are being transcribed by cyanobacteria in dead zones. We detected the highest number of N_2-fixation-related RNA transcripts in the oxic station A, possibly due to there being a higher relative abundance of cyanobacteria at that

station than at the hypoxic-anoxic stations. The sampled hypoxic-anoxic stations have low or no nitrate and nitrite (50), which explains why assimilatory nitrate reduction and uptake were prevalent only in the oxic sediment at station A. That N_2 fixation was possible in the dead zone sediment was indicated by the presence of *Dolichospermum*/*Anabaena* known to carry heterocysts to conduct N_2 fixation (7). Furthermore, non-heterocystous cyanobacteria such as certain *Synechococcus* species have also been described to conduct N_2 fixation (51). However, Baltic Sea dead zone sediments have been shown to be rich in ammonium (50), which is a favorable bioavailable source of nitrogen for some cyanobacteria (52). It is therefore possible that N_2 fixation was conducted inside specific microniches in the heterogenous sediment (such as biofilms or on/inside particles) where ammonium might have been scarce. However, further controlled studies are needed to investigate if cyanobacterial N_2 fixation is an important metabolic process in dead zone sediments. We were also able to detect RNA transcripts classified to genes coding for photosynthesis at all sampled stations. The highest number of photosynthesis RNA transcripts was detected at the oxic station A, possibly due to cyanobacteria having the highest relative abundance at that station. Accumulation of RNA transcripts attributed to the photosystem in darkness has previously been observed for the strain *Synechocystis* sp. strain PCC 6803 (53), and an increase in photosystem II units for *Anabaena variabilis* ATCC 2941 (25). Similarly to previous laboratory studies mentioned above, our data also indicate that heterotrophic cyanobacteria in dark anoxic sediments produce photosynthesis-related RNA transcripts.

We have here shown that cyanophages and cyanobacteria are present in one of the largest dead zones in the world. Cyanophages were detected at all stations and had a different beta diversity in the oxic sediment than in the hypoxic and anoxic sediments, suggesting that cyanobacteria and/or the environment select for specific cyanophages. Moreover, our results show that these cyanophages can infect cyanobacteria, affecting the photosystem and phosphate regulation. Top prevalent cyanobacteria detected include genera not capable of forming akinetes (*Cyanobium* and *Synechococcus*) and akinete-forming *Dolichospermum*/*Anabaena*. Cyanobacterial RNA transcripts in sediment were classified to, e.g., anaerobic glycolysis and N_2 fixation. Considering that large amounts of cyanobacteria sinking to dead zone sediments are known to fuel the benthic ecosystems with phosphorus (so-called internal loading), our cyanophage data indicate the potential for viral lysis of cyanobacteria, and this might sustain the high nutrient turnover in these heavily eutrophied environments.

MATERIALS AND METHODS

Study area and sampling. Sediment was collected using a modified box corer (54) during 23 to 26 April 2018 from four stations, located below the euphotic zone, following a water depth and oxygen gradient (stations A, D, E, and F) in the dead zone of Eastern Gotland basin, Baltic Sea (the stations and geochemical data have previously been presented in the work of Marzocchi et al. [55]) (Table 1; 2018 oxygen data first presented in the work of Broman et al. [33]). Three polyvinyl chloride (PVC) cylinders (5-cm diameter; 30-cm length) from each site were inserted into the box-core sediment and moved onto a sterile bench. The sediment was gently extruded, and the top 0 to 2 cm directly sliced into a 50-ml centrifuge tube. The sample was directly flash frozen and kept in liquid N_2 until being transferred and stored at −80°C.

Nucleic acid extraction. DNA and RNA were extracted from thawed and homogenized sediment with the DNeasy PowerMax soil kit (Qiagen) and RNeasy PowerSoil kit (Qiagen), with 10 g and 2 g input material, respectively. Extracted RNA was DNase treated with the Turbo DNA-free kit (Invitrogen) and rRNA depletion using the RiboMinus transcriptome isolation kit (bacterial version, ThermoFisher Scientific). Multiplexed libraries were prepared with the ThruPLEX DNA-seq (Rubicon Genomics) and TruSeq RNA Library Prep v2 [Illumina, without the poly(A) selection step] kits for DNA and RNA, respectively. Paired-end 2- by 150-bp sequencing was conducted at the Science for Life Laboratory, Stockholm, Sweden, on the Illumina NovaSeq platform (DNA on one lane, NovaSeq6000 S2, and RNA on one lane, Illumina NovaSeq6000 S4). The sequencing yielded on average 41 million (range 32 to 52) and 82 million (range 74 to 89) read-pairs for each DNA and RNA sample, respectively.

Bioinformatics. Illumina adapters were removed from the raw sequence data by using SeqPrep 1.2 (56) on default settings targeting the adapter sequences. Phi-X174 control sequences were removed from the data by mapping the reads with bowtie2 2.3.4.3 (57) against the PhiX genome (NCBI reference sequence: NC_001422.1). Reads were quality trimmed using Trimmomatic 0.36 (58) with the parameters

LEADING:20 TRAILING:20 MINLEN:50, yielding quality-trimmed reads with an average read length of 137 and 140 bp for the DNA and RNA data, respectively.

Metagenome and RNA-seq quality-trimmed sequences (Trimmomatic: paired without unpaired, PwU) were classified against the NCBI RefSeq genome database (downloaded 1 March 2019) using Kraken2 2.0.7 with a paired-end setup (59). The DNA data consisted on average of 103,043 reads mapped to cyanobacterial genes (range 51,939 to 152,036), while the RNA data consisted on average of 3,860,948 reads mapped to cyanobacterial genes (range 2,647,420 to 5,345,457). The RNA samples still contained on average 89% rRNA sequences (range 87 to 92%) after ribosomal depletion and therefore contained a large amount of rRNA alongside mRNA, and this likely helped to further identify the cyanobacterial community in the sediment. This method made it possible to classify a large amount of reads and detect cyanobacteria. However, because the reads classify against genes with different lengths in the RefSeq genomes, it is not possible to directly compare minor differences in relative abundances of taxonomic groups (although it gives a good indication of the distribution of reads). The final taxonomy data were analyzed and visualized as a relative proportion of classified reads (%) in the software Explicet 2.10.5 (60).

The DNA PwU quality-trimmed reads were used to construct a metagenome coassembly using MEGAHIT 1.1.2 on default settings (61). The Prokka 1.12 software tool (62) was used for gene prediction with Prodigal 2.6.3 (63) and annotation using BLAST 2.6.0+ (64) against the UniProtKB/Swiss-Prot database (database downloaded 31 January 2019) (65), with the parameters –-proteins uniprot_sprot.fasta –-metagenome. DNA and RNA PwU quality-trimmed reads were then mapped onto the coassembly using bowtie2 on default settings, and the output .sam files were converted to .bam with SAMtools 1.9 (66). Final sequence counts were estimated by using HTSeq-count from the HTSeq python package 0.9.1 (67) with the .bam files and PROKKA output .gff file as input, with the parameters -s no -f bam -t CDS -i ID. Sequence counts were normalized among samples as *g*ene length corrected *t*rimmed *m*ean of *M*-values (GeTMM) (68). Unique UniProtKB/Swiss-Prot identifiers were merged, and identifiers affiliated with cyanobacteria in the UniProtKB/Swiss-Prot database were extracted. The final data consisted on average of 175,134 mapped cyanobacterial DNA sequences per sample (range 143,600 to 209,247) and an average of 5,080 mapped cyanobacterial RNA transcripts per sample (range 4,075 to 6,048). Proteins were categorized into KEGG modules (69) by linking UniProtKB/Swiss-Prot identifiers to KEGG KO identifiers using the "Retrieve/ID mapping" function available on the official UniProt website, https://www.uniprot.org/uploadlists/.

Contigs longer than 2,000 bp in the metagenome coassembly were extracted using sqtek 1.3 and identified as viruses with VirSorter 1.0.3 (70) using the supplied RefseqABVir database on default settings via the CyVerse Discovery Environment interface (https://de.cyverse.org). Contigs classified as "Pretty sure" and "Quite sure" by VirSorter were used for further analyses. The contigs were classified for taxonomy using BLAST 2.10.1+ (64) against the NCBI NT database (data: 14 January 2021) with the following parameters: -max_target_seqs 5 -outfmt 6 -evalue 0.001 -task blastn. The first listed hit with the highest bit score was used for each contig. Open reading frames (ORFs) were detected in these contigs by using prodigal 2.6.3 on default settings (63). To predict potential cyanophages, network analysis with isolated genome-sequenced bacterial and archaeal viruses was conducted using vConTACT2 v0.9.8 with default settings (NCBI Bacterial and Archaeal Viral RefSeq V88 database [34]). vConTACT uses the Markov Cluster Algorithm (MCL) with an inflation value of 2 to cluster similar protein sequences (34). The ORFs were further classified using BLASTP 2.9.0+ against a database of all viral genomes from the NCBI RefSeq database (downloaded date: 12 July 2019) with the parameters -max_target_seqs 1 -outfmt 6 -evalue 0.001 to verify the cyanophages. Bowtie2 was used to map DNA PwU reads on the contigs and ORFs with a 90% identity alignment threshold. Considering the reads had an average length of 137 bp after quality trimming, using Bowtie2 parameters "–score-min L,0,-0.6." allows for 14 mismatches without including additional gap penalties. The output .sam files were converted to .bam and sorted by coordinates using SAMtools 1.9 (66). BEDTools 2.27.1 (71) was used to calculate total read depth per contig (mapped bp) and coverage per contig (%) using parameters "bedtools genomecov -d" and "bedtools genomecov -pc.", respectively. SAMtools idxstats were used to retrieve mapped counts of cyanophage ORFs for the DNA samples (no RNA reads could be mapped to the cyanophage ORFs). The data set was then delimited to cyanophage-identified contigs with a coverage of at least 75% to ensure the viral genome was present in the sample, following the protocols of previous ocean viral surveys (72). The amount of "mapped bp per contig" was normalized among samples by first dividing the mapped bp for each contig with the length of the contig (kb), followed by dividing with the total number of bases in the metagenome (Mb) (72). A full list of bioinformatic statistics is available in Data Set S5 in the supplemental material, such as number of reads obtained after sequencing, quality trimming, and mapping against the metagenome coassembly and numbers of reads classified against the UniProtKB/Swiss-Prot database.

Statistics. Shannon's H alpha diversity was calculated on the normalized sequence counts for the cyanophage contigs as well as their classified NCBI NT taxonomy (by summing counts with the same contig NCBI taxon identifier for each sample) using the software PAST 3.25 (73). Shannon's H alpha diversity index for the cyanobacteria was calculated in the software Explicet based on subsampling counts to the lowest sample size (2,647,420 counts) and bootstrap × 100 (with the mean reported as the final alpha index). Nonmetric multidimensional scaling (NMDS) showing Bray-Curtis beta diversity was based on the normalized counts for the cyanophage contigs and analyzed in the software PAST 3.25. NMDS plots of cyanobacterial community structure or cyanobacterial protein beta diversity with cyanophages as overlying triplot were constructed using the metaMDS function in the vegan R package (74). The best explanatory cyanophage for the cyanobacterial community structure was analyzed with the BVSTEP method (75) using R 3.6.0 (76) and the bvStep function with default settings in the sinkr R package (77).

The bvStep was run by using the distance methods Bray-Curtis for cyanobacterial proteins and Euclidean distances for cyanophages. Spearman correlations were conducted to find patterns between cyanophage contigs and cyanobacterial proteins by using the function rcorr in the Hmisc R package (78). Differences in alpha diversity between stations were tested with one-way ANOVAs and *post hoc* Tukey tests using IBM SPSS 26. Differences in the beta diversity between stations were tested with PERMANOVA (9,999 permutations) using the software PAST. Differences in RNA transcripts for annotated proteins between stations were tested with the R package edgeR 3.24.3 (79) by using the "run_DE_analysis.pl" script supplied with Trinity 2.8.2 (80). False-discovery rates (FDR) of <0.05 were used to indicate statistical significances.

Data availability. The raw sequencing data supporting the conclusions of this article are available in the NCBI BioProject repository, PRJNA531756 (81).

SUPPLEMENTAL MATERIAL

Supplemental material is available online only.

FIG S1, PDF file, 1.3 MB.

FIG S2, PDF file, 0.1 MB.

FIG S3, PDF file, 0.2 MB.

FIG S4, PDF file, 0.03 MB.

DATA SET S1, XLSX file, 0.2 MB.

DATA SET S2, XLSX file, 0.02 MB.

DATA SET S3, XLSX file, 0.1 MB.

DATA SET S4, XLSX file, 1.3 MB.

DATA SET S5, XLSX file, 0.01 MB.

ACKNOWLEDGMENTS

Individual financial support was provided by the Swedish Research Council Formas to S.B. (grant no. 2017-01513); the Swedish Research Council, Vetenskapsrådet to K.H. (grant no. 2013-4554); the Swedish Research Council VR to P.O.J.H. (grant no. 2015-03717); the Stockholm University strategic funds for Baltic Sea research to F.J.A.N.; the Swedish Environmental Protection Agency's Research (grant no. NV-802-0151-18) to F.J.A.N. in collaboration with the Swedish Agency for Marine and Water Management; and the Swedish Research Council Formas to F.J.A.N. (grant no. 2016-00804). This material is based upon work supported by the National Science Foundation under award numbers DBI-0735191, DBI-1265383, and DBI-1743442 (www.cyverse.org).

We acknowledge support from the National Genomics Infrastructure in Stockholm funded by Science for Life Laboratory, the Knut and Alice Wallenberg Foundation, and the Swedish Research Council, and from the SNIC/Uppsala Multidisciplinary Center for Advanced Computational Science for assistance with massively parallel sequencing and access to the UPPMAX computational infrastructure. We thank the captain and crew of University of Gothenburg R/V *Skagerak* for skillful support at sea.

E.B. drafted the manuscript and conducted laboratory work, bioinformatics, and data analyses. K.H. conducted bioinformatics and data analyses and gave feedback on the manuscript. S.B. sampled in the field, conducted sediment microprofiling, and gave feedback on the manuscript. P.O.J.H. led the sea expedition and gave feedback on the manuscript. F.J.A.N. coordinated the study and helped draft the manuscript. The research was designed by E.B., S.B., and F.J.A.N. All authors read and approved the final manuscript.

We declare that we have no competing interest.

REFERENCES

1. Suttle CA. 2007. Marine viruses—major players in the global ecosystem. Nat Rev Microbiol 5:801–812. https://doi.org/10.1038/nrmicro1750.
2. Waterbury JB, Valois FW. 1993. Resistance to co-occurring phages enables marine synechococcus communities to coexist with cyanophages abundant in seawater. Appl Environ Microbiol 59:3393–3399. https://doi.org/10.1128/AEM.59.10.3393-3399.1993.
3. Suttle CA, Chan AM. 1993. Marine cyanophages infecting oceanic and coastal strains of Synechococcus: abundance, morphology, cross-infectivity and growth characteristics. Mar Ecol Prog Ser 92:99–99. https://doi.org/10.3354/meps092099.
4. Sullivan MB, Waterbury JB, Chisholm SW. 2003. Cyanophages infecting the oceanic cyanobacterium Prochlorococcus. Nature 424:1047–1051. https://doi.org/10.1038/nature01929.
5. Cairns J, Coloma S, Sivonen K, Hiltunen T. 2016. Evolving interactions between diazotrophic cyanobacterium and phage mediate nitrogen release and host competitive ability. R Soc Open Sci 3:160839. https://doi.org/10.1098/rsos.160839.

6. Holmfeldt K, Titelman J, Riemann L. 2010. Virus production and lysate recycling in different sub-basins of the northern Baltic Sea. Microb Ecol 60:572–580. https://doi.org/10.1007/s00248-010-9668-8.
7. Castenholz RW. 2015. General characteristics of the cyanobacteria. *In* Trujillo ME, Dedysh S, DeVos P, Hedlund B, Kämpfer P, Rainey FA, Whitman WB (ed), Bergey's manual of systematics of archaea and bacteria. John Wiley & Sons, Inc, Hoboken, NJ.
8. Karlson AML, Duberg J, Motwani NH, Hogfors H, Klawonn I, Ploug H, Barthel Svedén J, Garbaras A, Sundelin B, Hajdu S, Larsson U, Elmgren R, Gorokhova E. 2015. Nitrogen fixation by cyanobacteria stimulates production in Baltic food webs. Ambio 44:413–426. https://doi.org/10.1007/s13280-015-0660-x.
9. Karlson AML, Nascimento FJA, Elmgren R. 2008. Incorporation and burial of carbon from settling cyanobacterial blooms by deposit-feeding macrofauna. Limnol Oceanogr 53:2754–2758. https://doi.org/10.4319/lo.2008.53.6.2754.
10. Brocke HJ, Wenzhoefer F, de Beer D, Mueller B, van Duyl FC, Nugues MM. 2015. High dissolved organic carbon release by benthic cyanobacterial mats in a Caribbean reef ecosystem. Sci Rep 5:8852. https://doi.org/10.1038/srep08852.
11. O'Neil JM, Roman MR. 1994. Ingestion of the cyanobacterium Trichodesmium spp. by pelagic harpacticoid copepods Macrosetella, Miracia and Oculosetella. Hydrobiologia 292:235–240.
12. Nascimento FJA, Karlson AM, Elmgren R. 2008. Settling blooms of filamentous cyanobacteria as food for meiofauna assemblages. Limnol Oceanogr 53:2636–2643. https://doi.org/10.4319/lo.2008.53.6.2636.
13. Scanlan DJ, West NJ. 2002. Molecular ecology of the marine cyanobacterial genera Prochlorococcus and Synechococcus. FEMS Microbiol Ecol 40:1–12. https://doi.org/10.1111/j.1574-6941.2002.tb00930.x.
14. Li X, Dreher TW, Li R. 2016. An overview of diversity, occurrence, genetics and toxin production of bloom-forming *Dolichospermum* (*Anabaena*) species. Harmful Algae 54:54–68. https://doi.org/10.1016/j.hal.2015.10.015.
15. Emeis KC, Struck U, Leipe T, Pollehne F, Kunzendorf H, Christiansen C. 2000. Changes in the C, N, P burial rates in some Baltic Sea sediments over the last 150 years - relevance to P regeneration rates and the phosphorus cycle. Mar Geol 167:43–59. https://doi.org/10.1016/S0025-3227(00)00015-3.
16. Stal LJ, Albertano P, Bergman B, Bröckel K, Gallon JR, Hayes PK, Sivonen K, Walsby AE. 2003. BASIC: Baltic Sea cyanobacteria. An investigation of the structure and dynamics of water blooms of cyanobacteria in the Baltic Sea—responses to a changing environment. Cont Shelf Res 23:1695–1714. https://doi.org/10.1016/j.csr.2003.06.001.
17. Conley DJ. 2012. Ecology: save the Baltic Sea. Nature 486:463–464. https://doi.org/10.1038/486463a.
18. Peinert R, Saure A, Stegmann P, Stienen C, Haardt H, Smetacek V. 1982. Dynamics of primary production and sedimentation in a coastal ecosystem. Netherlands J Sea Res 16:276–289. https://doi.org/10.1016/0077-7579(82)90036-9.
19. Fuchsman CA, Palevsky HI, Widner B, Duffy M, Carlson MCG, Neibauer JA, Mulholland MR, Keil RG, Devol AH, Rocap G. 2019. Cyanobacteria and cyanophage contributions to carbon and nitrogen cycling in an oligotrophic oxygen-deficient zone. ISME J 13:2714–2726. https://doi.org/10.1038/s41396-019-0452-6.
20. Vahtera E, Conley DJ, Gustafsson BG, Kuosa H, Pitkänen H, Savchuk OP, Tamminen T, Viitasalo M, Voss M, Wasmund N, Wulff F. 2007. Internal ecosystem feedbacks enhance nitrogen-fixing cyanobacteria blooms and complicate management in the Baltic Sea. Ambio 36:186–195.2.0.CO;2]. https://doi.org/10.1579/0044-7447(2007)36[186:IEFENC]2.0.CO;2.
21. Nascimento FJA, Karlson AML, Näslund J, Gorokhova E. 2009. Settling cyanobacterial blooms do not improve growth conditions for soft bottom meiofauna. J Exp Mar Biol Ecol 368:138–146. https://doi.org/10.1016/j.jembe.2008.09.014.
22. Middelburg JJ, Meysman FJR. 2007. Burial at sea. Science 316:1294–1295. https://doi.org/10.1126/science.1144001.
23. Diaz RJ, Rosenberg R. 2008. Spreading dead zones and consequences for marine ecosystems. Science 321:926–929. https://doi.org/10.1126/science.1156401.
24. Kaplan-Levy RN, Hadas O, Summers ML, Rücker J, Sukenik A. 2010. Akinetes: dormant cells of cyanobacteria, p 5–27. *In* Lubzens E, Cerda J, Clark M (ed), Dormancy and resistance in harsh environments. Springer, New York, NY.
25. Mannan RM, Pakrasi HB. 1993. Dark heterotrophic growth conditions result in an increase in the content of photosystem ii units in the filamentous cyanobacterium *Anabaena variabilis* ATCC 29413. Plant Physiol 103:971–977. https://doi.org/10.1104/pp.103.3.971.
26. Pelroy RA, Bassham JA. 1972. Photosynthetic and dark carbon metabolism in unicellular blue-green algae. Arch Mikrobiol 86:25–38. https://doi.org/10.1007/BF00412397.
27. Richardson LL, Castenholz RW. 1987. Enhanced survival of the cyanobacterium *Oscillatoria terebriformis* in darkness under anaerobic conditions. Appl Environ Microbiol 53:2151–2158. https://doi.org/10.1128/AEM.53.9.2151-2158.1987.
28. Voss M, Dippner JW, Humborg C, Hürdler J, Korth F, Neumann T, Schernewski G, Venohr M. 2011. History and scenarios of future development of Baltic Sea eutrophication. Estuar Coast Shelf Sci 92:307–322. https://doi.org/10.1016/j.ecss.2010.12.037.
29. Bonaglia S, Klawonn I, De Brabandere L, Deutsch B, Thamdrup B, Brüchert V. 2016. Denitrification and DNRA at the Baltic Sea oxic–anoxic interface: substrate spectrum and kinetics. Limnol Oceanogr 61:1900–1915. https://doi.org/10.1002/lno.10343.
30. Hargreaves KR, Anderson NJ, Clokie MRJ. 2013. Recovery of viable cyanophages from the sediments of a eutrophic lake at decadal timescales. FEMS Microbiol Ecol 83:450–456. https://doi.org/10.1111/1574-6941.12005.
31. Cai L, Jørgensen BB, Suttle CA, He M, Cragg BA, Jiao N, Zhang R. 2019. Active and diverse viruses persist in the deep sub-seafloor sediments over thousands of years. ISME J 13:1857–1864. https://doi.org/10.1038/s41396-019-0397-9.
32. Bianchi TS, Engelhaupt E, Westman P, Andrén T, Rolff C, Elmgren R. 2000. Cyanobacterial blooms in the Baltic Sea: natural or human-induced? Limnol Oceanogr 45:716–726. https://doi.org/10.4319/lo.2000.45.3.0716.
33. Broman E, Bonaglia S, Holovachov O, Marzocchi U, Hall POJ, Nascimento FJA. 2020. Uncovering diversity and metabolic spectrum of animals in dead zone sediments. Commun Biol 3:106. https://doi.org/10.1038/s42003-020-0822-7.
34. Bolduc B, Jang HB, Doulcier G, You Z-Q, Roux S, Sullivan MB. 2017. vConTACT: an iVirus tool to classify double-stranded DNA viruses that infect Archaea and Bacteria. PeerJ 5:e3243. https://doi.org/10.7717/peerj.3243.
35. Vandieken V, Sabelhaus L, Engelhardt T. 2017. Virus dynamics are influenced by season, tides and advective transport in intertidal, permeable sediments. Front Microbiol 8:2526. https://doi.org/10.3389/fmicb.2017.02526.
36. Weinbauer MG, Brettar I, Höfle MG. 2003. Lysogeny and virus-induced mortality of bacterioplankton in surface, deep, and anoxic marine waters. Limnol Oceanogr 48:1457–1465. https://doi.org/10.4319/lo.2003.48.4.1457.
37. Taylor GT, Iabichella M, Ho T-Y, Scranton MI, Thunell RC, Muller-Karger F, Varela R. 2001. Chemoautotrophy in the redox transition zone of the Cariaco Basin: a significant midwater source of organic carbon production. Limnol Oceanogr 46:148–163. https://doi.org/10.4319/lo.2001.46.1.0148.
38. Barrangou R. 2015. The roles of CRISPR–Cas systems in adaptive immunity and beyond. Curr Opin Immunol 32:36–41. https://doi.org/10.1016/j.coi.2014.12.008.
39. Riemann L, Holmfeldt K, Titelman J. 2009. Importance of viral lysis and dissolved dna for bacterioplankton activity in a P-limited estuary, northern Baltic Sea. Microb Ecol 57:286–294. https://doi.org/10.1007/s00248-008-9429-0.
40. Gao EB, Huang Y, Ning D. 2016. Metabolic genes within cyanophage genomes: implications for diversity and evolution. Genes 7:80. https://doi.org/10.3390/genes7100080.
41. Kim SK, Makino K, Amemura M, Shinagawa H, Nakata A. 1993. Molecular analysis of the *phoH* gene, belonging to the phosphate regulon in *Escherichia coli*. J Bacteriol 175:1316–1324. https://doi.org/10.1128/jb.175.5.1316-1324.1993.
42. Ivanciuc T, Sbrana E, Ansar M, Bazhanov N, Szabo C, Casola A, Garofalo RP. 2016. Hydrogen sulfide is an antiviral and antiinflammatory endogenous gasotransmitter in the airways. Role in respiratory syncytial virus infection. Am J Respir Cell Mol Biol 55:684–696. https://doi.org/10.1165/rcmb.2015-0385OC.
43. Stal LJ, Moezelaar R. 1997. Fermentation in cyanobacteria. FEMS Microbiol Rev 21:179–211. https://doi.org/10.1016/S0168-6445(97)00056-9.
44. Thureborn P, Franzetti A, Lundin D, Sjöling S. 2016. Reconstructing ecosystem functions of the active microbial community of the Baltic Sea oxygen depleted sediments. PeerJ 4:e1593. https://doi.org/10.7717/peerj.1593.
45. Jessen GL, Lichtschlag A, Ramette A, Pantoja S, Rossel PE, Schubert CJ, Struck U, Boetius A. 2017. Hypoxia causes preservation of labile organic matter and changes seafloor microbial community composition (Black Sea). Sci Adv 3:e1601897. https://doi.org/10.1126/sciadv.1601897.
46. Hulthe G, Hulth S, Hall POJ. 1998. Effect of oxygen on degradation rate of refractory and labile organic matter in continental margin sediments.

Geochim Cosmochim Acta 62:1319–1328. https://doi.org/10.1016/S0016-7037(98)00044-1.
47. Hallenbeck PC, Kochian LV, Benemann JR. 1981. Hydrogen evolution catalyzed by hydrogenase in cultures of cyanobacteria. Z Naturforsch C 36:87–92. https://doi.org/10.1515/znc-1981-1-217.
48. Sukenik A, Rücker J, Maldener I. 2019. Dormant cells (akinetes) of filamentous cyanobacteria demonstrate a great variability in morphology, physiology, and ecological function, p 65–77. In Mishra AK, Tiwari DN, Rai AN (ed), Cyanobacteria. Academic Press, New York, NY.
49. Callieri C, Slabakova V, Dzhembekova N, Slabakova N, Peneva E, Cabello-Yeves PJ, Di Cesare A, Eckert EM, Bertoni R, Corno G, Salcher MM, Kamburska L, Bertoni F, Moncheva S. 2019. The mesopelagic anoxic Black Sea as an unexpected habitat for Synechococcus challenges our understanding of global "deep red fluorescence." ISME J 13:1676–1687. https://doi.org/10.1038/s41396-019-0378-z.
50. Hall POJ, Almroth Rosell E, Bonaglia S, Dale AW, Hylén A, Kononets M, Nilsson M, Sommer S, van de Velde S, Viktorsson L. 2017. Influence of natural oxygenation of Baltic proper deep water on benthic recycling and removal of phosphorus, nitrogen, silicon and carbon. Front Mar Sci 4:27. https://doi.org/10.3389/fmars.2017.00027.
51. Bergman B, Gallon JR, Rai AN, Stal LJ. 1997. N_2 fixation by non-heterocystous cyanobacteria. FEMS Microbiol Rev 19:139–185. https://doi.org/10.1016/S0168-6445(96)00028-9.
52. Domingues RB, Barbosa AB, Sommer U, Galvão HM. 2011. Ammonium, nitrate and phytoplankton interactions in a freshwater tidal estuarine zone: potential effects of cultural eutrophication. Aquat Sci 73:331–343. https://doi.org/10.1007/s00027-011-0180-0.
53. Smart LB, McIntosh L. 1991. Expression of photosynthesis genes in the cyanobacterium Synechocystis sp. PCC 6803: psaA-psaB and psbA transcripts accumulate in dark-grown cells. Plant Mol Biol 17:959–971. https://doi.org/10.1007/BF00037136.
54. Blomqvist S, Ekeroth N, Elmgren R, Hall PO. 2015. Long overdue improvement of box corer sampling. Mar Ecol Prog Ser 538:13–21. https://doi.org/10.3354/meps11405.
55. Marzocchi U, Bonaglia S, van de Velde S, Hall POJ, Schramm A, Risgaard-Petersen N, Meysman FJR. 2018. Transient bottom water oxygenation creates a niche for cable bacteria in long-term anoxic sediments of the Eastern Gotland Basin. Environ Microbiol 20:3031–3041. https://doi.org/10.1111/1462-2920.14349.
56. St John J. 2011. SeqPrep. https://github.com/jstjohn/SeqPrep.
57. Langmead B, Salzberg SL. 2012. Fast gapped-read alignment with Bowtie 2. Nat Methods 9:357–359. https://doi.org/10.1038/nmeth.1923.
58. Bolger AM, Lohse M, Usadel B. 2014. Trimmomatic: a flexible trimmer for Illumina sequence data. Bioinformatics 30:2114–2120. https://doi.org/10.1093/bioinformatics/btu170.
59. Wood DE, Salzberg S. 2014. Kraken: ultrafast metagenomic sequence classification using exact alignments. Genome Biol 15:R46. https://doi.org/10.1186/gb-2014-15-3-r46.
60. Robertson CE, Harris JK, Wagner BD, Granger D, Browne K, Tatem B, Feazel LM, Park K, Pace NR, Frank DN. 2013. Explicet: graphical user interface software for metadata-driven management, analysis and visualization of microbiome data. Bioinformatics 29:3100–3101. https://doi.org/10.1093/bioinformatics/btt526.
61. Li D, Luo R, Liu CM, Leung CM, Ting HF, Sadakane K, Yamashita H, Lam TW. 2016. MEGAHIT v1.0: a fast and scalable metagenome assembler driven by advanced methodologies and community practices. Methods 102:3–11. https://doi.org/10.1016/j.ymeth.2016.02.020.
62. Seemann T. 2014. Prokka: rapid prokaryotic genome annotation. Bioinformatics 30:2068–2069. https://doi.org/10.1093/bioinformatics/btu153.
63. Hyatt D, Chen GL, Locascio PF, Land ML, Larimer FW, Hauser LJ. 2010. Prodigal: prokaryotic gene recognition and translation initiation site identification. BMC Bioinformatics 11:119. https://doi.org/10.1186/1471-2105-11-119.
64. Altschul SF, Gish W, Miller W, Myers EW, Lipman DJ. 1990. Basic local alignment search tool. J Mol Biol 215:403–410. https://doi.org/10.1016/S0022-2836(05)80360-2.
65. The UniProt Consortium. 2019. UniProt: a worldwide hub of protein knowledge. Nucleic Acids Res 47:D506–D515. https://doi.org/10.1093/nar/gky1049.
66. Li H, Handsaker B, Wysoker A, Fennell T, Ruan J, Homer N, Marth G, Abecasis G, Durbin R, 1000 Genome Project Data Processing Subgroup. 2009. The sequence alignment/map format and SAMtools. Bioinformatics 25:2078–2079. https://doi.org/10.1093/bioinformatics/btp352.
67. Anders S, Pyl PT, Huber W. 2015. HTSeq–a Python framework to work with high-throughput sequencing data. Bioinformatics 31:166–169. https://doi.org/10.1093/bioinformatics/btu638.
68. Smid M, Coebergh van den Braak RRJ, van de Werken HJG, van Riet J, van Galen A, de Weerd V, van der Vlugt-Daane M, Bril SI, Lalmahomed ZS, Kloosterman WP, Wilting SM, Foekens JA, IJzermans JNM, the MATCH Study Group, Martens JWM, Sieuwerts AM. 2018. Gene length corrected trimmed mean of M-values (GeTMM) processing of RNA-seq data performs similarly in intersample analyses while improving intrasample comparisons. BMC Bioinformatics 19:236. https://doi.org/10.1186/s12859-018-2246-7.
69. Kanehisa M, Goto S. 2000. KEGG: Kyoto encyclopedia of genes and genomes. Nucleic Acids Res 28:27–30. https://doi.org/10.1093/nar/28.1.27.
70. Roux S, Enault F, Hurwitz BL, Sullivan MB. 2015. VirSorter: mining viral signal from microbial genomic data. PeerJ 3:e985. https://doi.org/10.7717/peerj.985.
71. Quinlan AR, Hall IM. 2010. BEDTools: a flexible suite of utilities for comparing genomic features. Bioinformatics 26:841–842. https://doi.org/10.1093/bioinformatics/btq033.
72. Brum JR, Ignacio-Espinoza JC, Roux S, Doulcier G, Acinas SG, Alberti A, Chaffron S, Cruaud C, de Vargas C, Gasol JM, Gorsky G, Gregory AC, Guidi L, Hingamp P, Iudicone D, Not F, Ogata H, Pesant S, Poulos BT, Schwenck SM, Speich S, Dimier C, Kandels-Lewis S, Picheral M, Searson S, Bork P, Bowler C, Sunagawa S, Wincker P, Karsenti E, Sullivan MB, Tara Oceans Coordinators. 2015. Patterns and ecological drivers of ocean viral communities. Science 348:1261498. https://doi.org/10.1126/science.1261498.
73. Hammer Ø, Harper DAT, Ryan PD. 2001. PAST: paleontological statistics software package for education and data analysis. Palaeontol Electron 4:9.
74. Oksanen J, Blanchet FG, Kindt R, Legendre P, O'Hara R, Simpson GL, Solymos P, Stevens MHH, Szoecs E, Wagner H. 2018. vegan: community ecology package. R package version 2.5-2.
75. Clarke K, Warwick R. 1998. Quantifying structural redundancy in ecological communities. Oecologia 113:278–289. https://doi.org/10.1007/s004420050379.
76. R Core Team. 2013. R: a language and environment for statistical computing. R Foundation for Statistical Computing, Vienna, Austria. http://www.R-project.org/.
77. Taylor M. 2017. sinkr: collection of functions with emphasis in multivariate data analysis. R package version 0.6.
78. Harrell FE, Jr, Dupont C. 2008. Hmisc: Harrell miscellaneous. R package version 3.
79. Robinson MD, McCarthy DJ, Smyth GK. 2010. edgeR: a Bioconductor package for differential expression analysis of digital gene expression data. Bioinformatics 26:139–140. https://doi.org/10.1093/bioinformatics/btp616.
80. Haas BJ, Papanicolaou A, Yassour M, Grabherr M, Blood PD, Bowden J, Couger MB, Eccles D, Li B, Lieber M, Macmanes MD, Ott M, Orvis J, Pochet N, Strozzi F, Weeks N, Westerman R, William T, Dewey CN, Henschel R, Leduc RD, Friedman N, Regev A. 2013. De novo transcript sequence reconstruction from RNA-seq using the Trinity platform for reference generation and analysis. Nat Protoc 8:1494–1512. https://doi.org/10.1038/nprot.2013.084.
81. Broman E, Holmfeldt K, Bonaglia S, Hall POJ, Nascimento FJA. 2020. Eastern Gotland Basin sediment DNA and RNA data. https://www.ncbi.nlm.nih.gov/bioproject/PRJNA531756.